Analyst

Enhanced DNA Detection Using a Multiple Pulse Pumping Scheme with Time-Gating (MPPTG)

Journal:	*Analyst*
Manuscript ID	AN-ART-01-2018-000136.R1
Article Type:	Paper
Date Submitted by the Author:	04-Apr-2018

Complete List of Authors:	Kimball, Joseph; Texas Christian Universityity, Physics and Astronomy Maliwal, Badri; University of North Texas Health Science Center, Molecular Biology and Immunology Raut, Sangram; University of North Texas Health Science Center, Institute of Cardiovascular and Metabolic Disease Doan, Hung; Texas Christian Universityity, Physics and Astronomy Nurekeyev, Zhangatay; Texas Christian University, Physics and Astronomy Gryzcynski, Ignacy; UNT Health Science Center, Molecular Biology and Immunology, Center for the Commercialization of Fluorescence Technology Gryczynski, Zygmunt; University of North Texas Health Science Center, Molecular Biology and Immunology

Enhanced DNA Detection Using a Multiple Pulse Pumping Scheme with Time-Gating (MPPTG)

Joseph D. Kimball[ǂ], Badri Maliwal[ǂ], Sangram L. Raut[€], Hung Doan[ǂ], Zhangatay Nurekeyev[ǂ], Ignacy Gryczynski[§], Zygmunt Gryczynski[ǂ*]

[ǂ] Department of Physics and Astronomy, Texas Christian University, 2800 S. University Dr. Fort Worth, Texas, 76129

[€] Department of Physiology and Anatomy, UNT Health Science Center, 3500 Camp Bowie Blvd, Fort Worth, Texas, 76107

[§] Institute for Molecular Medicine, Program in Fluorescence Technologies at the Center for Cancer Research, UNT Health Science Center, 3500 Camp Bowie Blvd, Fort Worth, Texas, 76107

ABSTRACT: Fluorescence signal enhancement induced by the binding of intercalators to DNA has been broadly utilized in various DNA detection methods. In most instances the increase in fluorescence intensity is associated with a concomitant increase of fluorescence lifetime. This increase of the fluorescence lifetime presents an additional opportunity to increase detection sensitivity. In this paper, we present a new approach to significantly enhance the sensitivity in detecting minute DNA concentrations. The approach is based on simultaneous use of time-gated detection and multi-pulse pumping. By using a calibrated burst of short pulses we highly enhance the contribution of long-lived fluorescence species, thus enabling easy time-gated detection. Using a classic DNA intercalator - Ethidium Bromide (EtBr) as an example with our novel multi-pulse pumping and time-gated detection technique, we were able to increase detection sensitivity over 70-fold with only 3 pulse excitation. This approach is generic and can be used with any analytical probe (exhibiting about 10 times change in lifetime) that shows an increase in fluorescence signal and fluorescence lifetime upon binding to a target.

Introduction

The signal-to-noise ratio (SNR) is the key factor that determines detection sensitivity in biomedical assays[1]. Using highly purified reagents that reduce background contribution, fluorescence technology can reliably detect single molecules. However, in real physiological conditions background from scattering, autofluorescence, and electronic noise raises the detection limit in most cases to high nanomolar concentrations and in the case of live cells or tissues even to micromolar range. Significant efforts are being directed towards development of brighter dyes that increase photon output from the chromophore to improve detection sensitivity. Brightness is a product of a dye's extinction coefficient and quantum yield. Many dyes at our disposal today have a brightness approaching the theoretical limit and any significant improvement is unlikely. More recently, plasmonic technology[2-4] and metal enhanced fluorescence presented the possibility for significant signal enhancements (over 1000 fold) but the enhancement only occurs in very close proximity to metallic nanostructure (up to 20 nm) and is not fluorophore specific (enhancement for fluorophore of interest and any proximal impurities are frequently comparable). This increases the overall photon flux but does not improve SNR in any relevant biological assay conditions. In addition, due to difficulties in controlling the structure uniformity of metallic nanostructures the enhancements are typically non-uniform on an assay platform, thus leading to additional ambiguity in detection.

Fluorescence-based methods are among preferred approaches for DNA detection offering high sensitivity, speed, and good specificity. The DNA intercalators (dyes that insert between bases of double-stranded DNA (dsDNA) and exhibit a change in fluorescence signal) have been widely utilized[5-7]. The approach takes advantage of the signal enhancement of dye emission (eventually also a shift of emission spectrum) upon intercalation within the DNA double helix. Such enhancement is due to dye stabilization within the dsDNA environment and lowering the non-radiative deactivation pathways resulting in a significant increase of the dye's quantum yield and a concomitant increase in its fluorescence lifetime. We now realize that the longer fluorescence lifetime for an intercalator bound to DNA opens up additional possibilities to further increase the detection sensitivity. Background components like scattering or Raman scattering are instantaneous processes (zero fluorescence lifetime) and fluorescence of unbound intercalator or physiological byproducts (impurities) typically presents short fluorescence lifetimes in the nanosecond and sub-nanosecond range. Therefore, fluorescence response characterized with longer fluorescence lifetimes (> 15 ns) opens very attractive possibility for increasing the detection sensitivity by using time-gating approach. Time-gated detection has been widely utilized to suppress background when using emitters with very long luminescence lifetimes such as lanthanides[8-11]. Time-gating is a passive approach and when the fluorescence lifetime of the probe is not much longer than the background lifetime (few orders of magnitude), it leads to a significant loss of the probe signal. Using a gate delay to significantly limit the background contribution sacrifices a significant part of the probe's signal, thus making detection of lower quantities of analyte impossible, and thereby raising the

limit of detection. Here, opening/delay gate refers simply to starting the detection of fluorescence signal after a finite time following the excitation pulse (as shown in Figure 1). This time delay will depend on the fluorescence lifetime of the probe being used and for a probe lifetime of about 20 ns it will be in the nanosecond range; not difficult to achieve with simple electronics. On the other hand, time gating proves to be extremely useful for long-lived luminophores with lifetimes in microsecond to milliseconds range, such as lanthanides or metal-ligand complexes[10, 12].

Only recently we introduced a new approach where a single pulse is divided to a closely spaced burst of short pulses exciting the sample. As a result of such excitation a much higher population of excited molecules with long fluorescence lifetime can be generated. We call this technology multi-pulse pumping that in combination with time-gated detection (MPPTG) opens a new way to increase the signal of a long-lived fluorescence component and increase the detection sensitivity several orders of magnitude[13-15]. This technology has been used by us to improve sensitivity of fluorescence-based biomedical imaging and now we realize it can be used to highly enhance the signal in analytical assays as well. Herein we present a new approach combining multi-pulse pumping and time-gating (MPPTG) to detection of dsDNA. Using one of the most common intercalators (Ethidium Bromide – EtBr), we were able to increase the detection limit over 70 fold. This is a generic approach that can be used with any dye that presents an increase in fluorescence lifetime upon binding (EtBr homo-dimer and 8-Anilino 1-napthelene sulfonic acid binding to protein)[16-18] or dyes that inherently have longer lifetimes[19, 20]

Material and Methods

Spectroscopic Measurements

UV-Vis absorption measurements were made using a Cary 50 bio UV–visible spectrophotometer (Varian, Inc). All measurements were performed at room temperature in 1 x 1 cm quartz cuvettes and sample concentration with optical density kept below 0.1. Fluorescence emission and lifetime measurements were performed on a FluoTime 300 fluorescence lifetime spectrometer (Piqoquant, GmbH). Laser excitation was provided by a Supercontinuum WhiteLase SC-400 (Fianium, Ltd) through a triple quartz prism monochromator to choose an excitation light of 510 nm ±5 nm. Detection was made by an R3809U-50 micro-channel plate photomultiplier tube (Hamamatsu, Inc). The resolution of the time correlated single photon counting module was set to 4 ps/bin. The fluorescence intensity, I(t), was measured in the magic angle (54.7^0) condition then the fluorescence lifetimes were analyzed using FluoFit program (PicoQuant, Inc, Version 4.4). The fits were calculated using a multi-exponential fitting model.

$$I(t) = \sum_i \alpha_i e^{-t/\tau_i} \qquad 1$$

Where, α_i is the amplitude of the decay of the i^{th} component at time t and τ_i is the lifetime of the i_{th} component. The intensity weighted average lifetime τ_{Int} was calculated using following equation:

$$\tau_{Int} = \sum_i f_i \tau_i \quad \text{where} \quad f_i = \frac{\alpha_i \tau_i}{\sum_i \alpha_i \tau_i} \qquad 2$$

For multiple pulse experiments, the laser light was passed through an optical setup shown in the Figure 7 and is described in a section below. This set up helped us get 3 and 4 pulses with 3.2 ns separation between each of them.

Theoretical Considerations

Free EtBr in an aqueous buffer presents fluorescence lifetime of ~1.5 ns and when bound to DNA the fluorescence increases, with a concomitant spectral blue shift, and most importantly its fluorescence lifetime increases to over 20 ns. The increase of signal and the spectral shift has been widely utilized for DNA detection. But the increase in fluorescence lifetime is dramatic and remains an unutilized and unexplored area. However, this change in fluorescence lifetime correlated with an increase of rotational correlation time upon binding to dsDNA allows for the observation of anomalous anisotropy decays[21].

A longer fluorescence lifetime of the EtBr bound to dsDNA opens up an interesting new possibility to increase the sensitivity for detecting minute amounts of DNA present in the sample. Our novel approach based on bursts of pulses (in place of a single pulse) significantly increases the initial signal from long-lived components over short-lived components and background[13, 14] and thus lowers the detection limit for the long-lifetime fraction. Also, substantial build-up of a long-lived component fraction makes the use of time-gated detection much easier - leading to a substantial increase of SNR. To estimate potential enhancement in detection sensitivity, first we a present theoretical consideration of a probe (e.g. EtBr) binding to a target (like DNA). Consider a conventional experiment in a solution of probe binding to a target biomolecule where both fractions of free probe and bound probe are in equilibrium. For the purpose of our simulation we assume a single binding site where equilibrium will be given by:

$$\theta = \frac{(K_d + C_1 + C_2) - \left[(K_d + C_1 + C_2)^2 - 4C_1C_2\right]}{2C_1} \qquad 3$$

Where K_d is the dissociation constant, C_1 and C_2 concentrations of target (DNA) and probe (EtBr) respectively, and θ represents ratio of fraction of bound to unbound probe to a target. One needs to remember that a DNA strand will have multiple binding sites for EtBr and the number of binding sites will depend on the length or number of base pairs. Moving to multiple binding sites is a relatively straight-forward process [22, 23]. In a typical experiment, we usually excite a very small fraction of available dyes (both free and bound). The measured signal would reflect the ratio between bound and unbound EtBr fractions (θ). For very low (trace) concentrations of DNA the relative fraction of bound intercalator would be very small and even if the signal change upon binding is large, the DNA detection limit would be relatively high due to the low signal value. To lower the detection limit, EtBr homo-dimer molecules are frequently used for which binding affinity (and specificity) is much greater and increases bound fraction relative to the free (unbound) fraction[24, 25]. This improves the ratio between bound and unbound intercalators signal enhancement due to the dimeric form and increases the detection sensitivity. The limiting factor is still relative background contribution

that does not change and thus a small concentration (amount) of DNA is difficult to detect even when using the homodimers.

To increase the detection sensitivity, we need to realize what the factors that limit the detection . For very low DNA concentrations, we need to use a low intercalator concentration (to lower free EtBr contribution) and most importantly the is background signal from various reagents and electronic noise. Theyare very difficult to separate from the sample signal since they overlap with sample emission and/or are leaking through the filters and/or monochromator[26-28]. To limit the contribution from sample and buffer auto-fluorescence, high reagent purity is preliminary requisite. Besides residual reagent and buffer contributions, secondary artifacts like scattering and Raman scattering are difficult to avoid and may have a significant contribution [29]. Even when the background contributions from regents and scattering are limited, electronic noise such as the dark current of the detection system becomes a hurdle for detecting very minute probe concentrations[30]. A low concentration means low signal and at such conditions the dark current of the detector starts to play a significant role.

When binding of the probe to target/biomolecules results in fluorescence intensity and concomitant increase in fluorescence lifetime, this opens an additional opportunities for detection enhancement. For very long fluorescence lifetimes (like lanthanides) time-gated detection gives excellent results [31, 32] but when lifetime change is only an order of magnitude as compared to free probe and background, the benefits are limited unless we are willing to sacrifice a significant amount of the probe signal. The general rule is that the delay gate time needs to be significantly longer than fluorescence lifetime of the free probe and background component. To achieve significant suppression of signal from a free probe and/or background the delay gate time should be 4-5 times longer than the fluorescence lifetime of a free probe. Having a relatively long delay gate time opening as compared to the lifetime of the bound probe will also significantly limit the portion of detected signal from bound-probe. Since our goal is to detect the lowest possible DNA concentrations, the required EtBr concentration will also be low, thus limiting the overall fluorescence signal. In such cases even with highly purified reagents, the scattering and detector dark current will become obstacles in achieving the lower detection limit. A simple increase of laser power (pulse energy) would not help since the signal from all- background, scattering, bound, and unbound fractions, will increase in the same proportion (we assume used excitation power is far from saturation level).

In case of EtBr and DNA, we would like to specifically increase the signal from bound fraction (long-lived fraction) over the background from free (unbound) dye and other sample and electronic noise contributions. An ideal approach would be to exclusively excite only molecules that have long fluorescence lifetime, an approach impossible to realize in practice in case of EtBr-DNA sample. We realized now we can increase the contribution of long-lived fraction by applying a purposely designed pulse sequence (pulse burst). Using an approach based on multiple-pulse pumping and time-gated detection, we can very effectively expose the long-lived fluorescence species. Time-gated detection increases the ratio between long-lived fraction and short-lived fraction. The increase in this ratio depends on the lifetime difference and can be very significant for long delays. Multi-pulse pumping can significantly (few fold) increase the initial contribution (fraction) of the long-lived component. Combining both multi-pulse pumping and time-gated detection (MPPTG) can drastically increase (over 2 orders of magnitude) sensitivity of biomedical or chemical assays without sacrificing useful signal from long-lived components. To understand the concept let's consider two different excitation modes. A typical experiment where we excite a sample with continuous wave (CW) excitation or stream of pulses with repetition rate (RR) for which 1/RR or distance between two consecutive pulses is much longer than the longest lifetime component in the sample (a typical case in time-correlated single photon counting (TCSPC) detection). In this case, the total observed fluorescence intensity will only depend on average excitation light intensity. The advantage of pulsed excitation is it will allow us to use the time-gated mode by starting our observation at a given delay gate time as compared to the excitation pulse. As the delay gate time increases, the entire signal decreases but the relative ratio between long-lived and short-lived fractions increases. In Figure 1, we are presenting intensity decay of the system that has two decay components, one τ_s = 1.5 ns (tau short) and another τ_l = 20 ns (tau long) fluorescence lifetimes representative of free EtBr and bound EtBr. For simplicity, we assume that the initial steady-state intensities (area under the decay) are identical. For that to happen the initial intensity (amplitude fraction) of the short-lived component must be 13.33 times greater (the amplitude fraction is 13.33 fold larger). Obviously, with the perfect system, we will deal with a signal that only originates from the dye. However, when detecting very low concentrations (low-level signals) the background and dark current of the detector become major limiting factors. In steady-state detection, the detector is open all the time and in time-resolved measurements, the detector is open for a finite period of time between pulses (at least 4-5 times longer than the longest lifetime component). These two elements (background and dark counts) become real experimental limitations. Contribution from such elements depends on the sample and is very difficult to account for. The dark current and other instrumental factors will obviously depend on the instrumental system and experimental conditions. In general, we can arbitrarily assume that background contribution (the sample/buffer autofluorescence and dark current) is below 10% of the signal from the weakest component (initial signal of unbound EtBr signal). In practice, this means that during the time when the detector is open, the number of counts detected from the weakest contributor is more than 90% of the signal. At this point we will assume that auto-fluorescence of the sample has very short lifetime (shorter than free EtBr) and we will include both autofluorescence and scattering together with detector dark counts into the background signal. Starting the experiment integrated emission signal from free dye If(t) and cumulative contribution from background, B are equal. While adding DNA, the bound fraction will contribute with higher intensity (Ib(t)) and longer fluorescence lifetime (the overall intensity will be increasing). After pulse excitation, both the free and bound intensity fractions are time dependent (exponential decays) and the overall contribution of the background will depend on the integration time. Since the free and bound fractions of EtBr have significantly different lifetimes, the relative contribution of the free and bound fractions will depend on the delay gate time, *gd*. At any given concentration of DNA the equilibrium between free and bound EtBr in the sample is given by Eq. 1. We can calculate corresponding

integrated intensities If_{gd}, Ib_{gd}, and B_{gd} measured starting with delay gate time (gd) as follows:

$$If_{gd} = \int_{gd}^{gd+T}(1-\theta)If(t)dt\,; \quad Ib_{gd} = \int_{gd}^{gd+T}\theta Ib(t)dt\,; \quad B_{gd} = \int_{gd}^{gd+T}Bdt \qquad 4$$

Where T is total time detector is open for signal detection, θ represent the fraction of EtBr bound to DNA as a function of DNA concentration according to Eq.3. If_{gd} is intensity of free EtBr, Ib_{gd} is the intensity of the bound fraction, and B is the contribution from the background (includes impurities, and electronic noise). In our simulation, we assume the initial concentration of EtBr to be such that the total initial counts from free EtBr (no DNA) constitutes 95% of total signal (5% are background counts). Applying the delay gate time, the fluorescence intensity detected from free EtBr will decrease and we will consider gate delay times up to the time for which the signal from EtBr will be 3% or more compared to dark current counts integrated over the same detection time, T. This happens for a gate delay time of about 10 ns and in our experiments we will not use more than 10 ns gate delay time.

Total fluorescence intensity as a function of DNA concentration will be given by:

$$I_{gd} = If_{gd}(1-\theta) + Ib_{gd}\theta + B_{gd} \qquad 5$$

Figure 2a shows the predicted change in fluorescence intensity for different delay gate times. In Figure 2b we are presenting the normalized intensity change (ratio) of the initial intensity of free EtBr and background components. It is clear that with increasing delay gate time the dynamic range for binding curves quickly increases but total measured signal decreases. The relative dark counts contribution quickly increases and measurements of the initial intensity of EtBr becomes the limiting step for appropriate detection. By evaluating Figure 1 for 0 ns delay gate time (no gate) the background signal is only about 5% of the signal from the free EtBr. But already for delay time of 4.5 ns the signal is about 50% and for 8 ns the dark counts (background) signal approaches 90% of the total detected signal from free EtBr (black line). For longer gate delay times, the free EtBr signal (no DNA) approaches the baseline level and for delay times longer than 10 ns, the initial signal from free EtBr is less than 3% of the background that we consider to be too difficult to accurately measure in practice. It could be beneficial to optimize delay gate times for gate opening those results in maximal signal enhancement for different DNA saturations. The following equation helps us understand this,

$$E(\theta, gd) = \frac{If_{gd}(1-\theta)+Ib_{gd}\theta+B_{gd}}{If_0+B_0} \qquad 6$$

Where, $If_0 + B_0$ is the initial signal from free EtBr and background with 0 delay gate times. Figure 3 shows the dependence of the signal enhancement, E, as a function of delay gate time for 6 intermediate target-to-ligand ratios (representing concentrations of binding sites as compared to the initial concentration of ligand). For no DNA ($\theta = 0$) the initial signal is 1 and drops to 0.05 as gate delay time increases (black line practically close to 0 in Figure 3). Already in the target DNA concentration that results in 0.1:1 ratio of target to ligand (red line) we see a clear maximum that is very pronounced for higher DNA concentrations. For 1:1 ratio (pink) that represents 50% bound the relative intensity change is close to maximum and for ratio 2:1 approaches saturation and changing ratio to 90:1 (dark blue) produces only minimal improvement. While in the presence of DNA, as the delay gate time increases the signal from both, free and bound decreases and the signal ratio between the bound and free quickly increases and reaches a maximum at about a ~9 ns delay. Since thebackground contribution is practically constant for any delay gate time and signal level from free fractions quickly decreases to background level, the ratio stops increasing at delays 8-9 ns and slowly decreases thereafter. As the DNA concentration increases, the dynamic range quickly increases approaching values close to 200 at maximum for higher bound fraction of EtBr. For a very long delay gate time (much longer than fluorescence lifetime of bound fraction) this ratio approaches 1. It is clear that for selected conditions the delay gate opening time of about 9 ns will give a best dynamic range that is almost 15 fold larger than that for a typical steady-state measurement (no gate). It is important to realize that we assumed substantial background signal and just by limiting the background contributions, the signal enhancement increases many folds.

To enhance the contribution of long-lived component we can introduce the pulse bursts excitation method as proposed[13,14]. By now applying time-gated detection we can significantly expand the dynamic range for signal change as a function of DNA concentration. Readers are encouraged to read other papers published by our group to get in-depth understanding of the theory behind MPPTG technology[13, 14]. We will use the same procedure for a single pulse and for multi-pulse (burst) excitation scheme. Supplementary Figure 1 shows the pulse burst scheme with intensity decays of short-lived and long - lived probes. For burst excitation, we will start the detection after the last pulse in the burst. Figure 5 shows the normalized intensity as a function of DNA concentration (represented by ratio of DNA binding sites to ligand concentration) as calculated from Eq. 5 for four pulse excitation and gate time opening 4 ns, 6 ns, and 10 ns. For comparison in Figure 4, we also included single pulse (steady-state) with no gate and 4 pulses with no gate applied. It is clear that 4 pulse excitation and 10 ns gate gives us a dynamic range of over 550 as compared to ~13 for normal steady-state excitation. This is over 42-fold enhancement as compared to a typical experiment.

Results and Discussion

To test our theoretical predictions we used commercially available EtBr and calf thymus DNA. We are aware that this DNA has multiple binding sites and simple equilibrium described by Equation 3 will need to be appropriately adjusted. But our objective is to prove that using multi-pulse excitation and time-gated detection we can greatly improve detection limits without sacrificing probe signal.

Figure 5 (a) shows the emission spectra of free 2μM EtBr and EtBr bound to DNA (40μM) and Figure 5 (b) presents intensity decays measured for free and DNA-bound EtBr at 610 nm observation (20 nm slit). As expected upon binding the intensity increase is almost 13-fold and the fluorescence lifetime changed from 1.5 ns to over 20 ns.

To test our assumption we generated 3 and 4 pulse bursts with pulse-to-pulse separation within the burst of 3.2 ns which is equivalent to a laser repetition rate of ~320 MHz. From theoretical predictions we would expect an over 2-fold increase in the long-lived fraction contribution when exciting with the 3-pulse burst. To generate bursts we used simple approach as schematically shown in Figure 6. A single pulse from a laser source is partially reflected (about 10%) by glass slide (G1) and 90% is transmitted through the glass G2 where about 10% is reflected and remaining 90% is transmitted to G3. The pulses are combined with corresponding glasses G' to pass on the same trajectory. To generate 4 and more pulses we need to add additional glasses. Each consecutive pulse travels extra 2a distance yielding relative delay. Neutral density filters (F) are used to regulate relative pulse intensities to achieve a burst of pulses of equal peak intensities. This simple approach allows us to form a burst of three or four pulses with intensities of about 6%-10% of the original pulse. But with 4 and more pulses the intensity of each pulse in the burst drops. Commercially available laser diodes can go up to 80 MHz repetition rate only. As developing and manufacturing a laser system with high (over 200 MHz repetition rate) repetition rate is a very expensive and time consuming enterprise, our approach in contrast is a simple and convenient way to form pulse bursts of higher repetition rate. Most laser diodes available today offer higher power output; sufficient to excite even a low concentration of compounds such as EtBr which has low extinction coefficient. Moreover, our current efforts are directed towards designing an optical fiber which will generate multiple pulses without significant loss of power. This will further increase the fluorescence enhancement and rate at which we collect the data.

We tested the signal increase induced by DNA using a fixed concentration of EtBr of 2μM with series of DNA additions. The results are presented in Figure 7. We started DNA titration from 94 nM DNA for which a clear increase (~20%) in the steady-state signal can be detected (Figure 7a) that corresponds to about 2% EtBr bound to DNA. We kept increasing the DNA concentration up to 660 nM for which we have about 10% EtBr bound to DNA and the intensity signal increases over 100% as compared to free EtBr. In the middle panel of Figure 7, we are presenting time-resolved intensity decays for various DNA concentrations with single pulse excitation. Figure 7c shows time-resolved intensity decays for 3 pulse burst excitation. The increase in long-lifetime component is clearly evident when going from 1 pulse to 3 pulse excitation. To numerically compare results, we first integrated the area under the decay curve for each DNA addition with a single pulse and 3 pulse excitation. Since the excitation pulse width is negligible (50-60 ps) as compared to the entire decay, the integration starts 50 ps after the peak (last peak for 3 pulse excitation) and extends for 150 ns (time much longer than the longest 20 ns lifetime component). Such integrated intensity decay corresponds to steady-state intensity. In Table 1, we present total photon output or total intensity compared to free EtBr intensity for various DNA concentrations. Also in Table 1, we present normalized integrated intensity decays (area under the decay curve) for 1 and 3 pulse excitations. While change in the total intensity with different DNA concentrations for single pulse excitation will correspond to observed steady-state intensity (from emission spectra measurement). However, the intensity change with three pulse excitation results in the overall change of over 2 times greater. We also performed the integration while applying time gating strategy for measured intensity decays. In the two following columns, we present integrated intensity decays when applying delay gate time of 10 ns. As theoretically predicted, the measured changes are much greater. With 3-pulse excitation and 10 ns gate delay time, the signal change going from free EtBr to 10% DNA bound EtBr sample increases almost ~80 fold as compared to only 2-fold increase for steady-state measurements.

To test potential limits for detection we used much lower DNA concentration (~20 nM) that leads to negligible (undetectable) change in steady-state fluorescence. We analyzed the sample intensity decays using 1, 2, 3, and 4-pulse excitation. Such a low DNA concentration yields only 0.5% of EtBr bound to DNA. In Figure 8a, we present intensity decays for 1, 2, 3, and 4 pulse excitations using the configuration analogical to that shown in Figure 6. Already visual inspection of intensity decay in Figure 8a indicates measurable change in the long-fraction contribution.

To more precisely estimate the contribution of long-lived component we conducted a lifetime analysis using a tail fit routine[33, 34]. A tail-fit routine allows to fit experimental data without pulse consideration (pulse deconvolution) starting the analysis at any time after the pulse. By shifting the delay for data analysis we only consider later photons limiting the contribution of fast decaying species. Such analysis is equivalent to time gating but the advantage is that this analysis accounts for background and results are fit to thousands of experimental points in the intensity decay. In Table S1 (Supplementary Information) we present results for the fit starting with the delay of 50 ps after peak (last peak in multi-pulse excitation), 0.5ns, 1ns, 3ns, 6ns, 8ns and 10 ns after the last peak. The integration window is kept constant to 100 ns. Recovered fluorescence lifetimes and their amplitude fractions are presented in Table S1. In Figure 8b, we present the recovered intensity amplitude for long lifetime component (middle panel) and short lifetime component (8c). The detectable fraction of long-lived component increases with the number of pulses and time gate delay. The long component fraction for 4 pulses excitation and 50 ps delay is 1.08 and it increases to almost 68 for 10 ns gate time, thus reflecting an over 65-fold increase. In the same time the short fraction drops from over 98 for 50 ps delay to almost 31 for 10 ns gate delay time reflecting a 3 fold decrease. The relative combined change when considering the change in long and short components is almost 200. We also want to stress that these are results from a fitted data and the error in this routine is much smaller.

Conclusions

We presented EtBr-DNA as model case for ligand-biomolecule binding-type interactions. Overall results demonstrated the increase of fluorescence lifetime of the probe upon binding presents a new opportunity for significant increase of detection sensitivity by using multi-pulse excitation and time-gated detection (MPPTG). Use of multi-pulse technology allows for the increase (many fold) of the initial signal from long-lived components making time-gated detection much more effective. Presented example of EtBr binding to DNA results in about 13-fold increase in fluorescence signal and by taking advantage of the lifetime change from 1.5 ns to over 20

ns we could reliably increase the detection sensitivity to almost 70 fold without a significant signal loss. This approach can be used with any system that presents a similar change like other DNA inercalators or ANS binding to a globular protein. This technology can be applied to enhance the detection limits of commercially available immunoassays provided we can use the detection antibody labelled with long fluorescence lifetime dyes such as AzaDiOxaTriAngulenium (ADOTA) and Ruthenium.

ASSOCIATED CONTENT

Supporting Information

(Word Style "TE_Supporting_Information"). A listing of the contents of each file supplied as Supporting Information should be included. For instructions on what should be included in the Supporting Information as well as how to prepare this material for publication, refer to the journal's Instructions for Authors.

The Supporting Information is available free of charge on the ACS Publications website.

AUTHOR INFORMATION

Corresponding Author

* Zygmunt Gryczynski (z.gryczynski@tcu.edu)

Author Contributions

The manuscript was written through contributions from all authors. All authors have given approval to the final version of the manuscript.

ACKNOWLEDGMENT

This work is supported by RO1EB12003, R21EB017985 and NSF CBET 1403226.

REFERENCES

1. Frangioni, J. V. Molecular imaging. 2009, 8, 7290.2009. 00033.
2. Aslan, K.; Gryczynski, I.; Malicka, J.; Matveeva, E.; Lakowicz, J. R.; Geddes, C. D. Curr.Opin.Biotechnol. 2005, 16, 55-62.
3. Geddes, C. D.; Cao, H.; Gryczynski, I.; Gryczynski, Z.; Fang, J.; Lakowicz, J. R. The Journal of Physical Chemistry A. 2003, 107, 3443-3449.
4. Malicka, J.; Gryczynski, I.; Lakowicz, J. R. Biochem.Biophys.Res.Commun. 2003, 306, 213-218.
5. LePecq, J.; Paoletti, C. J.Mol.Biol. 1967, 27, 87-106.
6. Nafisi, S.; Saboury, A. A.; Keramat, N.; Neault, J.; Tajmir-Riahi, H. J.Mol.Struct. 2007, 827, 35-43.
7. Kelly, J. M.; Tossi, A. B.; McConnell, D. J.; OhUigin, C. Nucleic Acids Res. 1985, 13, 6017-6034.
8. Condrau, M. A.; Schwendener, R. A.; Niederer, P.; Anliker, M. Cytometry. 1994, 16, 187-194.
9. Dai, Z.; Tian, L.; Ye, Z.; Song, B.; Zhang, R.; Yuan, J. Anal.Chem. 2013, 85, 11658-11664.
10. Jin, D.; Piper, J. A. Anal.Chem. 2011, 83, 2294-2300.
11. Xiao, Y.; Zhang, R.; Ye, Z.; Dai, Z.; An, H.; Yuan, J. Anal.Chem. 2012, 84, 10785-10792.
12. Periasamy, A.; Siadat-Pajouh, M.; Wodnicki, P.; Wang, X.; Herman, B. USA Microsc.Anal. 1995, 3
13. Rich, R. M.; Gryczynski, I.; Fudala, R.; Borejdo, J.; Stankowska, D. L.; Krishnamoorthy, R. R.; Raut, S.; Maliwal, B. P.; Shumilov, D.; Doan, H. Methods. 2014, 66, 292-298.
14. Shumilov, D.; Rich, R. M.; Gryczynski, I.; Raut, S.; Gryczynski, K.; Kimball, J.; Doan, H.; Sørensen, T. J.; Laursen, B. W.; Borejdo, J. Methods and Applications in Fluorescence. 2014, 2, 024009.
15. Raut, S.; Rich, R.; Fudala, R.; Kokate, R.; Kimball, J.; Borejdo, J.; Vishwanatha, J.; Gryczynski, Z.; Gryczynski, I. Curr.Pharm.Biotechnol. 2014,
16. Gaugain, B.; Barbet, J.; Oberlin, R.; Roques, B. P.; Le Pecq, J. B. Biochemistry (N.Y.). 1978, 17, 5071-5078.
17. Glazer, A. N.; Peck, K.; Mathies, R. A. Proc.Natl.Acad.Sci.U.S.A. 1990, 87, 3851-3855.
18. Hawe, A.; Sutter, M.; Jiskoot, W. Pharm.Res. 2008, 25, 1487-1499.
19. Maliwal, B. P.; Fudala, R.; Raut, S.; Kokate, R.; SÃ¸rensen, T. J.; Laursen, B. W.; Gryczynski, Z.; Gryczynski, I. PloS one. 2013, 8, e63043.
20. Raut, S.; Fudala, R.; Rich, R.; Kokate, R.; Chib, R.; Gryczynski, Z.; Gryczynski, I. Nanoscale. 2014, 6, 2594-2597.
21. Chib, R.; Raut, S.; Sabnis, S.; Singhal, P.; Gryczynski, Z.; Gryczynski, I. Methods and Applications in Fluorescence. 2014, 2, 015003.
22. Ruedas-Rama, M. J.; Orte, A.; Crovetto, L.; Talavera, E. M.; Alvarez-Pez, J. M. The Journal of Physical Chemistry B. 2009, 114, 1094-1103.
23. Markovits, J.; Roques, B. P.; Le Pecq, J. Anal.Biochem. 1979, 94, 259-264.
24. Denhardt, D. T.; Kato, A. C. J.Mol.Biol. 1973, 77, 479IN7491-490494.
25. Rye, H. S.; Quesada, M. A.; Peck, K.; Mathies, R. A.; Glazer, A. N. Nucleic Acids Res. 1991, 19, 327-333.
26. Benson, R. C.; Meyer, R. A.; Zaruba, M. E.; McKhann, G. M. J.Histochem.Cytochem. 1979, 27, 44-48.
27. Roederer, M.; Murphy, R. F. Cytometry. 1986, 7, 558-565.
28. Rich, R. M.; Stankowska, D. L.; Maliwal, B. P.; Sørensen, T. J.; Laursen, B. W.; Krishnamoorthy, R. R.; Gryczynski, Z.; Borejdo, J.; Gryczynski, I.; Fudala, R. Analytical and bioanalytical chemistry. 2013, 405, 2065-2075.
29. Vedvik, K. L.; Eliason, H. C.; Hoffman, R. L.; Gibson, J. R.; Kupcho, K. R.; Somberg, R. L.; Vogel, K. W. Assay and drug development technologies. 2004, 2, 193-203.
30. Waters, J. C. J.Cell Biol. 2009, 185, 1135-1148.
31. Soini, E.; Kojola, H. Clin.Chem. 1983, 29, 65-68.
32. Johansson, M. K.; Cook, R. M.; Xu, J.; Raymond, K. N. J.Am.Chem.Soc. 2004, 126, 16451-16455.
33. Gregor, I.; Enderlein, J. Photochemical & Photobiological Sciences. 2007, 6, 13-18.
34. Jiménez-Banzo, A.; Ragas, X.; Kapusta, P.; Nonell, S. Photochemical & Photobiological Sciences. 2008, 7, 1003-1010.

Insert Table of Contents artwork here

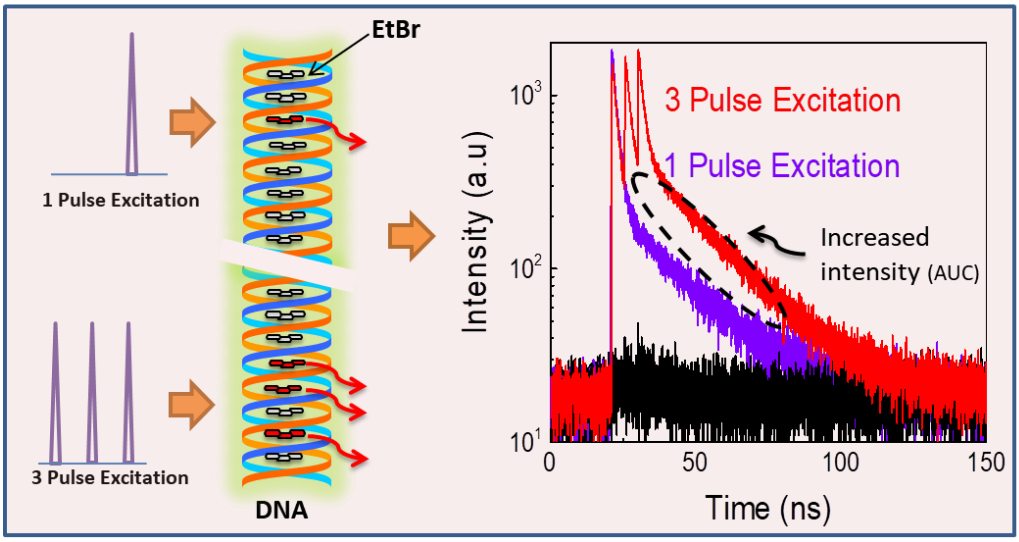

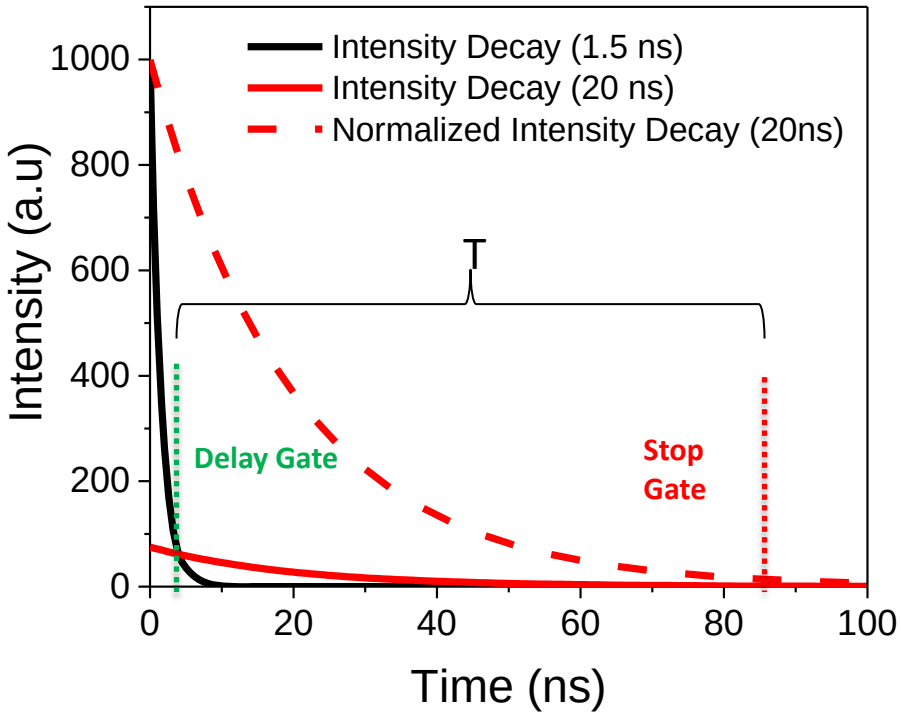

Figure 1: Simulated intensity decays for two lifetime probes 1.5ns (black) and 20ns (red) and dashed red line shows normalized 20ns probe decay.

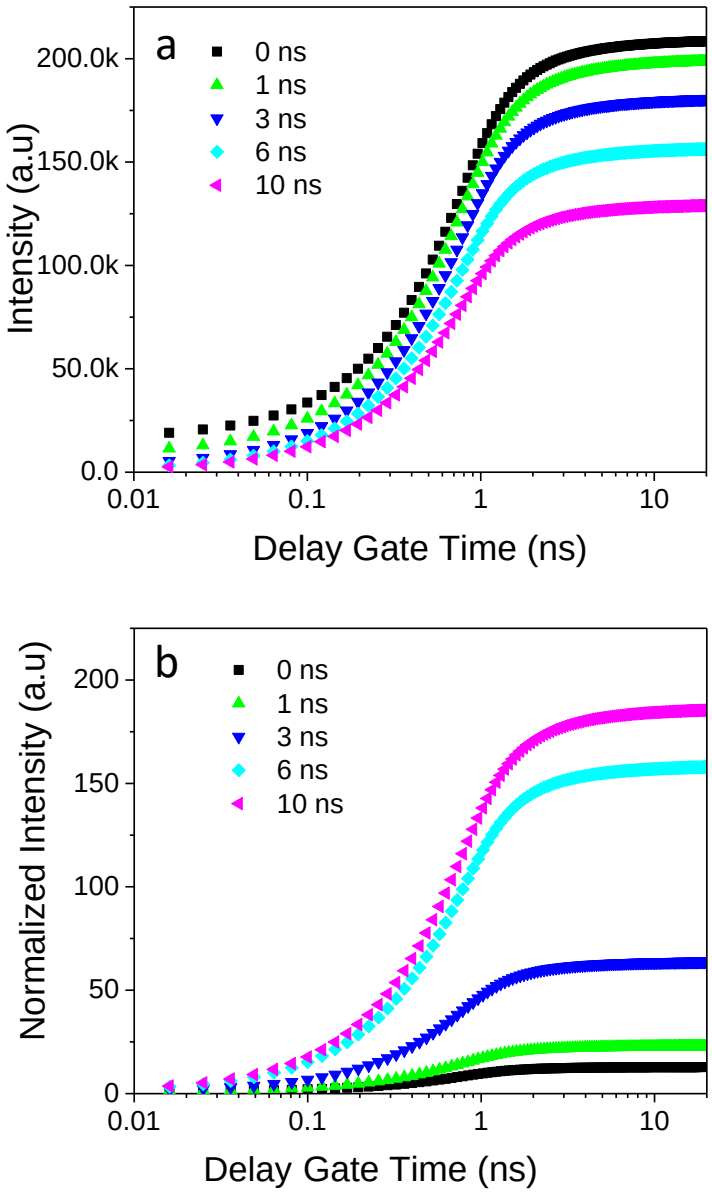

Figure 2: Figure 2a shows predicted change in fluorescence intensity for different gate opening times and figure 2b shows normalized intensity change for different gate opening times.

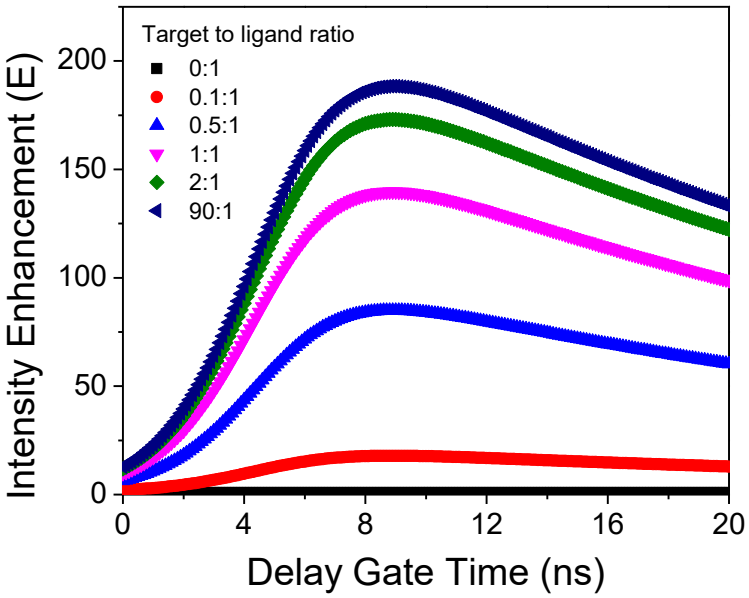

Figure 3: Dependence of signal or intensity enhancement on different gate times for different target to ligand ratio.

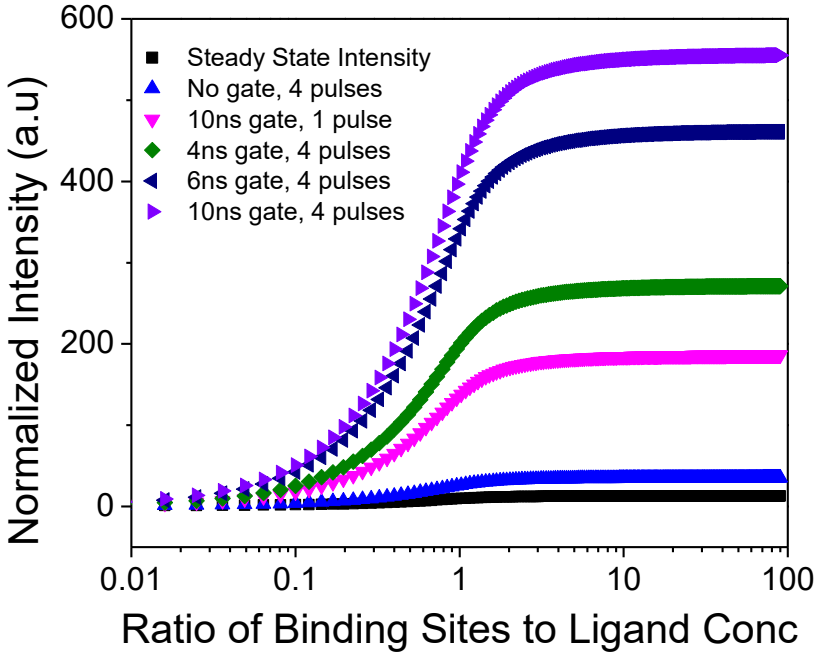

Figure 4: Normalized intensity for different ratio of DNA binding site to ligand concentration

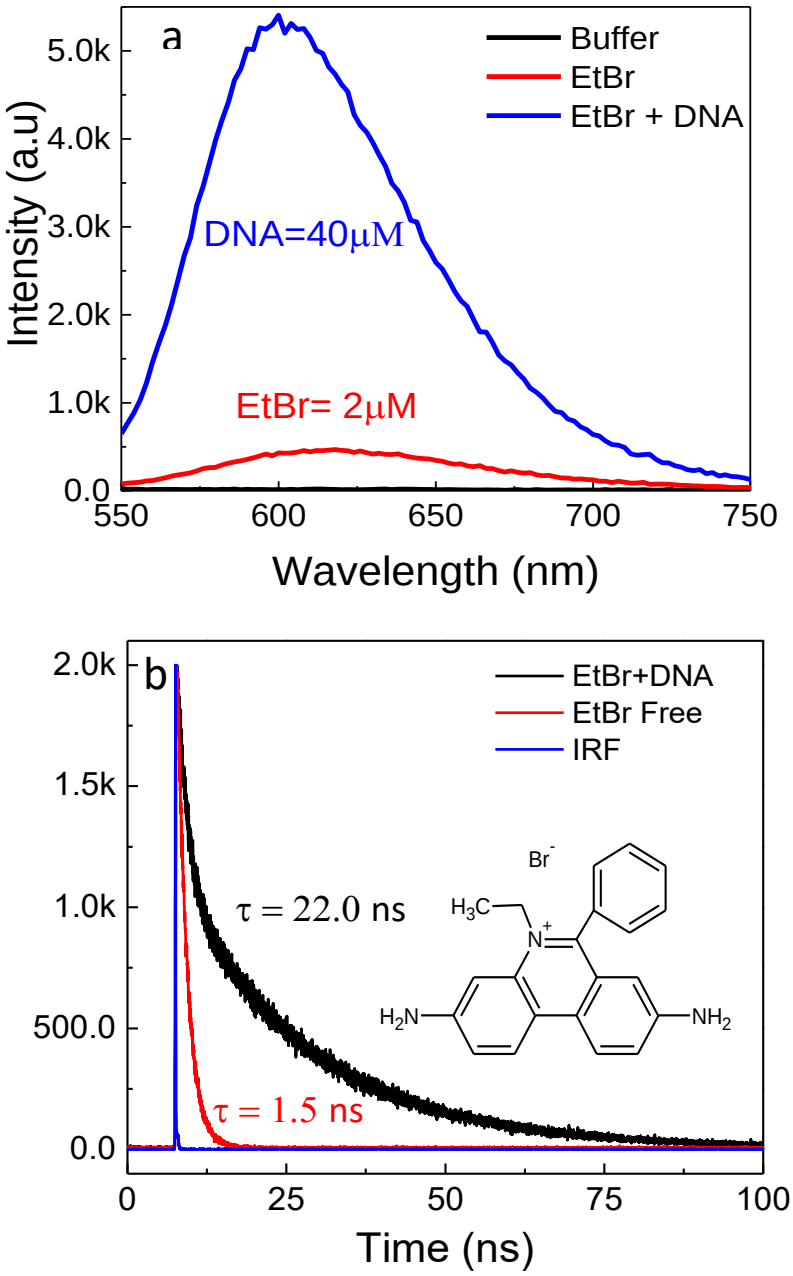

Figure 5: (a) Shows the emission spectra of free EtBr and bound to 40uM DNA. (b) Shows the respective fluorescence intensity decays for free and bound EtBr along with chemical structure of EtBr molecule.

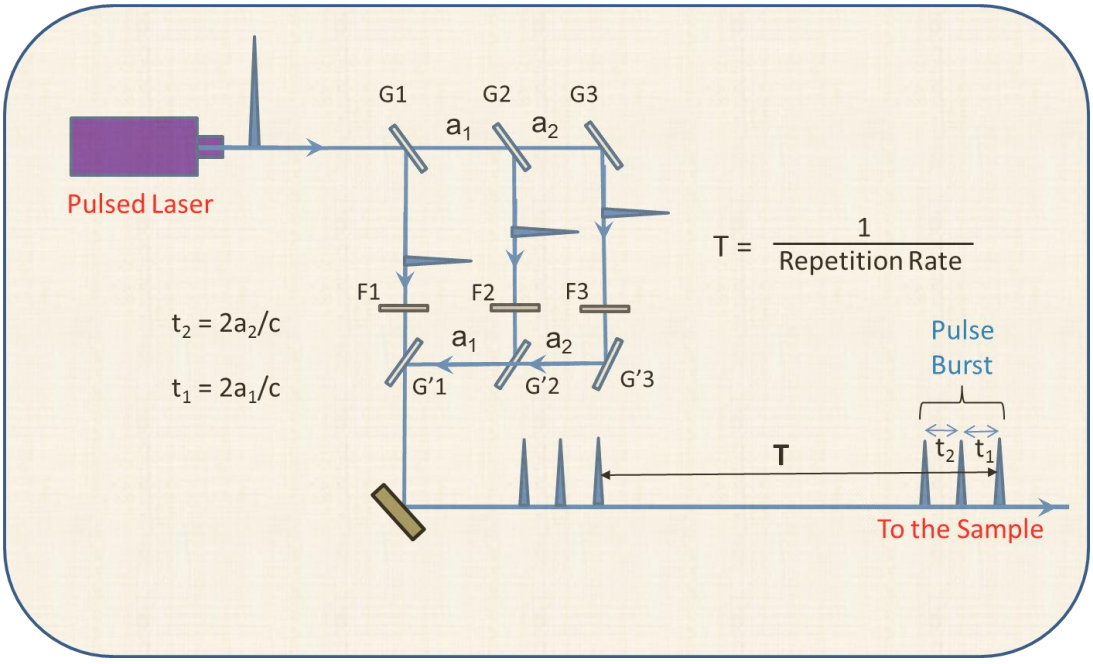

Figure 6: Schematics of multiple pulse generation using a single laser and different optical components.

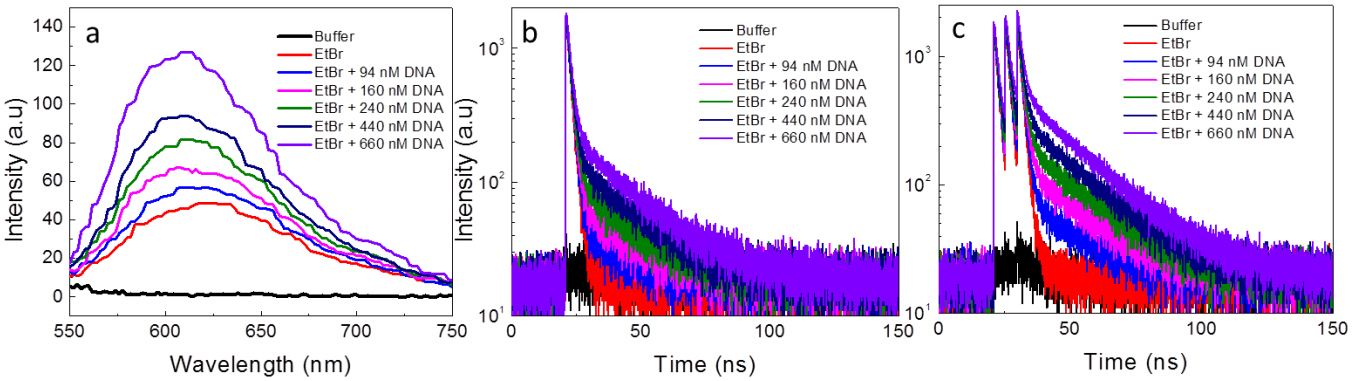

Figure 7: Left panel (a) shows the emission spectra of EtBr only and with different DNA concentrations (94 nM to 660 nM). Middle panel (b) shows the intensity decays for all samples from left panel using 1 pulse excitation. Right panel(c) shows the intensity decays of all the samples from left panel using 3 pulses excitation.

DNA [nM]	No Gate			10 ns Gate	
	Steady State	1 Pulse	3 Pulses	1 Pulse	3 Pulses
94	1.16	1.14	1.25	6.60	9.60
160	1.34	1.25	1.51	11.9	19.5
240	1.57	1.38	1.81	20.2	31.8
440	1.83	1.59	2.24	30.7	47.6
660	2.30	1.96	2.98	48.5	74.2

Table 1: Normalized intensity change compared to free EtBr intensity using multiple pulses and time gating.

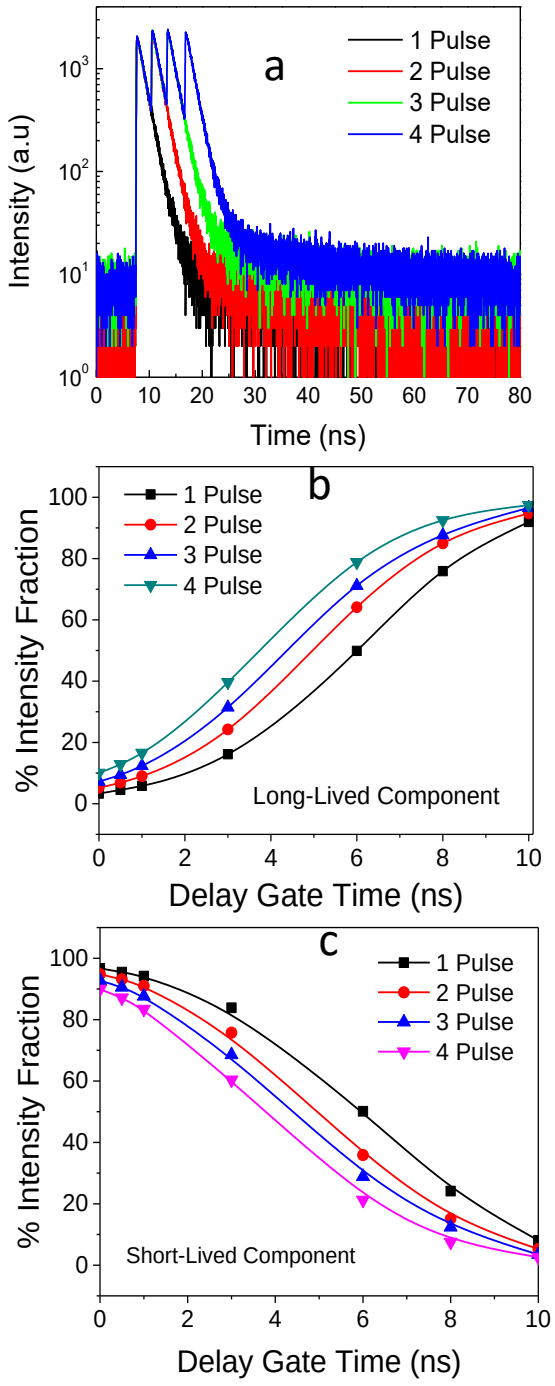

Figure 8: (a) shows the intensity decays for EtBr bound to 20nM DNA concentration. (b) shows the dependence of long-lived intensity fraction on different gate opening times. (c) shows the dependence of short-lived intensity fraction on different gate opening times.

SUPPLEMENTARY INFORMATION

Enhanced DNA Detection Using a Multiple Pulse Pumping Scheme with Time-Gating (MPPTG)

Joseph D. Kimball[‡], Badri Maliwal[‡], Sangram L. Raut[€], Hung Doan, Zhangatay Nurekeyev[‡], Ignacy Gryczynski[§], Zygmunt Gryczynski[‡*]

[‡] Department of Physics and Astronomy, Texas Christian University, 2800 S. University Dr. Fort Worth, Texas,76129

€ Department of Physiology and Anatomy, UNT Health Science Center, 3500 Camp Bowie Blvd, Fort Worth, Texas, 76107

[§] Institute for Molecular Medicine, Program in Fluorescence Technologies at the Center for Cancer Research, UNT Health Science Center, 3500 Camp Bowie Blvd, Fort Worth, Texas, 76107

Figure S1: Concept of multiple pulse excitation and effect on intensity of probes with different lifetimes

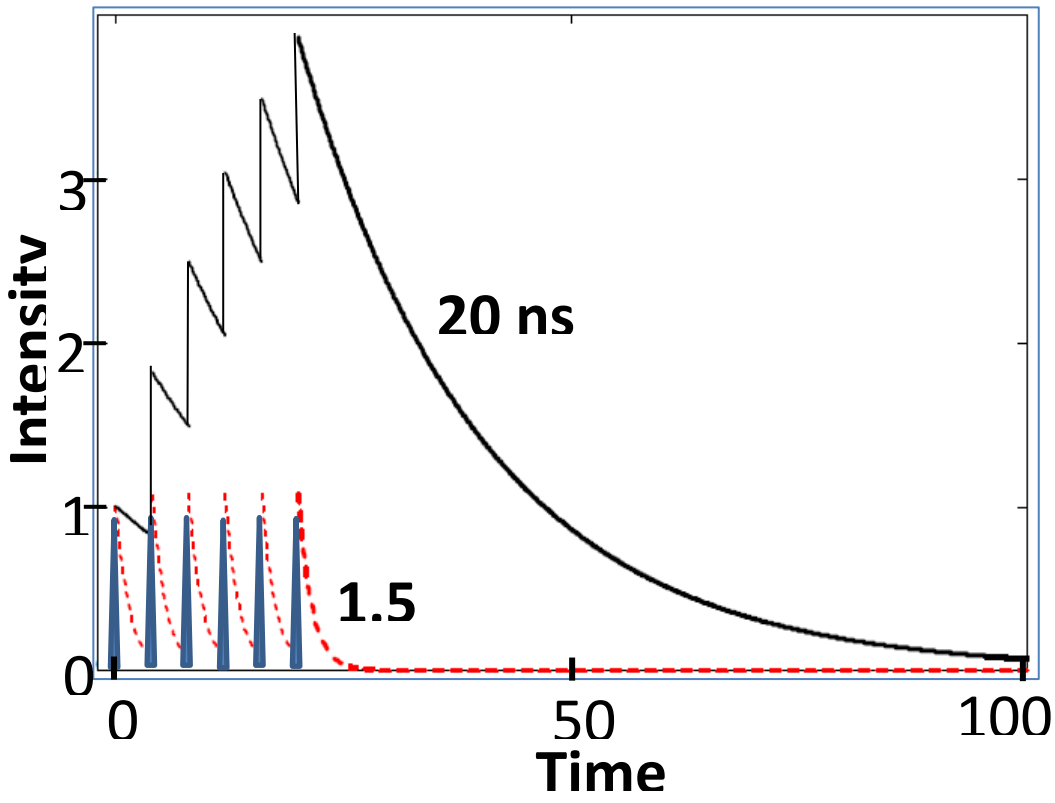

SUPPLEMENTARY INFORMATION

Tables :S1 Shows the amplitude weighted analysis of fluorescence intensity decays collected for 20nM DNA concentration for 1,2,3 and 4 uM EtBr concentrations.

50 ps delay calculation

Sample	α_1 (%)	α_2 (%)	τ_1 (ns)	τ_2 (ns)	Avg τ_{int} (ns)	Avg τ_{amp} (ns)	χ^2
1 pulse	0.52	99.48	13.46	1.55	2.07	1.61	0.85
2 pulse	0.64	99.36	17.46	1.54	2.62	1.65	0.81
3 pulse	0.95	99.05	16.57	1.53	2.95	1.67	0.97
4 pulse	1.08	98.92	19.95	1.54	3.81	1.74	0.94

0.5 ns delay calculation

Sample	α_1 (%)	α_2 (%)	τ_1 (ns)	τ_2 (ns)	Avg τ_{int} (ns)	Avg τ_{amp} (ns)	χ^2
1 pulse	0.54	99.46	13.40	1.55	2.08	1.61	0.85
2 pulse	0.66	99.34	17.49	1.54	2.66	1.65	0.81
3 pulse	0.96	99.04	16.60	1.53	2.96	1.67	0.97
4 pulse	1.13	98.87	19.97	1.54	3.91	1.75	0.94

1 ns delay calculation

Sample	α_1 (%)	α_2 (%)	τ_1 (ns)	τ_2 (ns)	Avg τ_{int} (ns)	Avg τ_{amp} (ns)	χ^2
1 pulse	0.65	99.35	13.94	1.56	2.24	1.64	0.84
2 pulse	0.89	99.11	17.65	1.55	3.04	1.70	0.80
3 pulse	1.28	98.72	16.74	1.53	3.42	1.73	0.97
4 pulse	1.51	98.49	20.05	1.54	4.61	1.82	0.94

3 ns delay calculation

Sample	α_1 (%)	α_2 (%)	τ_1 (ns)	τ_2 (ns)	Avg τ_{int} (ns)	Avg τ_{amp} (ns)	χ^2
1 pulse	1.98	98.02	14.11	1.56	3.50	1.81	0.84
2 pulse	2.74	97.26	18.45	1.58	5.75	2.04	0.80
3 pulse	3.89	93.11	17.88	1.58	6.70	2.21	0.97
4 pulse	4.71	95.29	20.86	1.57	9.21	2.48	0.93

SUPPLEMENTARY INFORMATION

6 ns delay calculation

Sample	α_1 (%)	α_2 (%)	τ_1 (ns)	τ_2 (ns)	Avg τ_{int} (ns)	Avg τ_{amp} (ns)	χ^2
1 pulse	9.08	90.92	15.49	1.64	8.37	2.90	0.83
2 pulse	13.76	86.24	19.21	1.68	13.00	4.10	0.80
3 pulse	18.05	81.95	18.93	1.67	13.98	4.80	0.96
4 pulse	21.42	78.39	21.42	1.58	17.21	5.87	0.94

8 ns delay calculation

Sample	α_1 (%)	α_2 (%)	τ_1 (ns)	τ_2 (ns)	Avg τ_{int} (ns)	Avg τ_{amp} (ns)	χ^2
1 pulse	28.35	76.15	14.90	1.55	11.57	4.74	0.83
2 pulse	30.85	69.15	18.50	1.46	15.93	6.72	0.78
3 pulse	40.32	59.68	19.31	1.81	17.18	8.87	0.96
4 pulse	47.84	52.16	21.28	1.59	19.80	11.01	0.94

10 ns delay calculation

Sample	α_1 (%)	α_2 (%)	τ_1 (ns)	τ_2 (ns)	Avg τ_{int} (ns)	Avg τ_{amp} (ns)	χ^2
1 pulse	49.41	50.59	14.56	1.33	13.43	7.86	0.83
2 pulse	62.49	37.51	18.74	1.70	17.86	12.35	0.77
3 pulse	58.07	41.93	17.95	0.86	17.38	10.79	0.96
4 pulse	68.54	31.46	21.19	1.23	20.67	14.91	0.94